

This paper was recommended for publication in revised form by Regional Editor Somchai Wongwises

PERFORMANCE AND FLOW DISTRIBUTION OF THE PLATE HEAT EXCHANGER WITH SUPERCRITICAL FLUID OF CARBON DIOXIDE

Chen-Xi Zhu

Department of mechanical engineering,
National Chiao Tung University,
Hsinchu, Taiwan 300

***Chi-Chuan Wang**

Department of mechanical engineering,
National Chiao Tung University,
Hsinchu, Taiwan 300

Yi-Chun Tang

Department of mechanical engineering,
National Chiao Tung University,
Hsinchu, Taiwan 300

Keywords: Supercritical fluid; plate heat exchanger; carbon dioxide; flow distribution

** Corresponding author: C.C. Wang, E-mail: ccwang@mail.nctu.edu.tw*

ABSTRACT

The present study proposes a plate heat exchanger model that is capable of simulating the supercritical fluids like CO₂. The plate heat exchanger is of U-type configuration, and the size of the plate is 600 mm wide and 218 mm in height. Simulations are carried out for both isothermal and non-isothermal cases with water-to-water and water-to-CO₂ plate heat exchanger. The proposed model was first compared with some existing water-to-water plate heat exchanger data. Generally, the predicted water flow distributions are in line with the experimental data. Yet the simulation results of temperature distribution alongside the plate agree excellently with other predicted model. For the water side distribution within the plate heat exchanger, it is found that a detectable mal-distribution prevails and the flowrate shows a consistent decline from the first to the last plate. Basically, a larger mal-distribution is seen when the inlet flowrate is increased or when the plate number is increased. The simulation indicates that the inlet temperature of water casts negligible influence on the water flowrate distribution. By contrast, it is found that the inlet temperature difference for the CO₂ side may raise significant changes of thermodynamics and transport property of CO₂, and result in a great difference in flow distribution. Generally the mal-distribution of the CO₂ is much less severe due to more even pressure difference between the intake and exhaust manifold. The effect of pressure on heating capacity for the water-CO₂

plate heat exchanger also depends on the ratio of heat capacity flow.

NOMENCLATURE

A	Cross-sectional area (m ²)
A _w	Effective heat transfer area (channel) (m ²)
C	heat capacity rate (J/K)
C _p	Heat capacity (J/kg·K)
C _t	coefficient of turning loss from inlet (-)
C _{to}	coefficient of turning loss from outlet (-)
D	inlet and outlet diameter (m)
D _h	hydraulic diameter (m)
D _e	equivalent diameter (m)
f	Dracy friction factor (-)
h	heat transfer coefficient (W/m ² ·K)
K _L	coefficient of loss from intake conduit (-)
K _C	coefficient of loss from exhaust conduit (-)
l	length of grids, m per grid
L	length of plate (m)
m [·]	mass flow rate (kg/s)
n	number of channels
N	number of grids (-)
P	cross-sectional wet perimeter (m)
P _{in}	pressure of inlet (Pa)
P _{out}	pressure of outlet (Pa)
P _{ch}	pressure of channels (Pa)

ΔP_{ch}	pressure difference in channels (Pa)
t	plate thickness (m)
u_c	velocity in channel (m/s)
U	overall heat transfer coefficient ($W/m^2 \cdot K$)
v	velocity (m/s)
V_{in}	inlet velocity (m/s)
V_{out}	outlet velocity (m/s)
V_{ch}	velocity of channel (m/s)
V_{chm}	average velocity of channel (m/s)
w	width of plates, m
Z	direction from plate inlet to outlet (m)
z	dimensionless location of channel , $z = x/L$

Greek letters

β	ratio of channel velocity to mean velocity (-)
θ	dimensionless temperature (-)
τ_w	shear stress of wall (Pa)
v_c	dimensionless channel velocity ($= v_{ch}/V_{chm}$),
ζ_c	coefficient of total head loss in channels (-)

Superscript

*	ratio of heat capacity
---	------------------------

Subscript

c	channels
C	CO ₂ side
in/out	inlet/outlet
H	water side
i	number of channels
j	number of grids

INTRODUCTION

The plate heat exchangers feature compact size and high heat transfer performance, and is regarded to be more advantageous than its counterpart – shell-and-tube heat exchangers. Hence they are rapidly used to replace the traditional shell-and-tube heat exchangers in many industrial applications such as dairy, food processing, paper/pulp, heating, ventilating, and other related industry [1]. Appreciable experimental studies for single-phase flow in plate heat exchangers had been reported. For example, Khan et al. [2] had mentioned tens of experimental studies in association with single phase fluid. Yet Han et al. [3] also summarized more than fifteen numerical studies concerning plate heat exchangers applicable for single-phase fluid. However, the foregoing studies, either experimental or numerical, mainly stressed on the performance of single-phase fluids like water or air. The development of high-performance heat pump water heaters using natural working fluids had received a lot attention recently as far as energy conservation and greenhouse gas reduction is concerned [4]. Among the existing natural refrigerants, carbon dioxide (CO₂) is especially prominent for its outstanding features like nonflammable, nontoxic, no known carcinogenic, and free from mutagenic. Moreover, using CO₂ in refrigerating systems can be regarded as an alternative form of

carbon capture, thereby helping to relief the influence on climate change [5]. For the revival of CO₂ refrigeration system, the pioneering works of Lorentzen et al. [6-8] had proved that the use of CO₂ can meet the simultaneous needs for an efficient air-conditioning and for hot water production. This can be made available by operating the CO₂ system in the transcritical region [9]. Note that the critical state of carbon dioxide is at 7.8 MPa and 330 K, respectively. Therefore the heat exchanger is operated above the critical point and is known as a gas cooler. It should be mentioned that the physical properties of carbon dioxide vary drastically near the critical point, the conventional numerical simulation methods for plate heat exchanger are not applicable. As a consequence, the present study aims at the problem and seeks to include the tremendous change of physical properties such as density, viscosity and heat capacity. Since the physical properties of the carbon dioxide vary drastically at supercritical state, thus the tremendous changes of density and viscosity may impose changes of heat transfer performance and accordingly the corresponding flow distribution. For example, when temperature variation between the plates changes considerably, it will cause considerable maldistribution effect, and may affect the heat transfer performance appreciably.

Normally heat transfer characteristics of supercritical CO₂ can be regarded single-phase gas fluid, hence the famous Dittus-Boelter [10] and Gnielinski correlations [11] is roughly applicable in round tube. However, these correlations are mostly applicable to fluids having constant properties. Since CO₂ reveals significant change of property during trans-critical process. The applicability of these correlations may be limited and require deliberate examination. The departure between these correlations may become even pronounced when the temperature is close to the pseudo-critical point [12]. The horizontal pipe experiment conducted by Yoon et al. [13] reveals that change of density near the critical point has a dramatic effect on the heat transfer. The experiment conducted by Son et al. [14] also reported that the difference between the wall and center of the pipe can greatly affect the efficiency of heat transfer due to significant change in properties.

Bassiouny and Martin [15] presented a model to investigate the flow distribution of the plate heat exchangers. Meanwhile, the control volume for intake and exhaust conduit is also studied in this paper, it is assumed that the ratio of average velocity β is known and the friction loss of inlet is also negligible. In realistic cases, however, the value of β will change subject to different locations of intake and exhaust conduit. Rao et al. [16] proposed a one-dimensional model for predicting the heat transfer and flow distribution of a plate heat exchanger. However, until now, there is no model available for predicting the heat transfer characteristics of the trans-critical CO₂ in a plate heat exchanger, it is therefore the objective of this study to account for the drastic property change of CO₂ in a

plate gas cooler. Note that the significant change of physical property, especially heat capacity, may impose appreciable influence on the heat transfer performance. This can be made clear from Yu et al. [17, 18] who numerically and experimentally examined the transcritical heat transfer phenomenon of a tube-in-tube heat exchanger, and a local maximum is reported. Hence, it would be interested to study this phenomenon in the plate heat exchanger. Moreover, the plate heat exchangers normally consists many plates where maldistribution within the plates may occur and impair the heat transfer performance accordingly. Therefore, it is quite imperative to investigate the flow distribution and the associated heat transfer performance of the CO₂ plate heat exchangers.

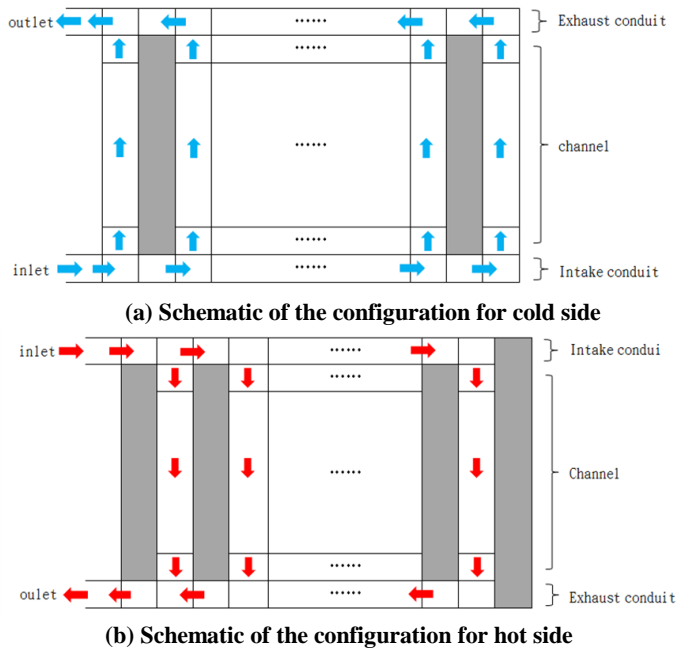


Fig. 1 Numerical modeling for the water-CO₂ plate heat exchanger.

NUMERICAL MODELING AND CALCULATION

The simulation considers a one-dimensional flow for water or CO₂ alongside the plate. The plate heat exchanger is of U-type configuration, i.e. the inlet and outlet for water or CO₂ are located at the first plate. Heat lost from the plate heat exchanger to the ambient is negligible and the effect of gravity is also neglected. As depicted in Fig. 1(a), the plate heat exchanger is consisted of cold plate (water side) and hot plate (CO₂) and the layout configuration of plate heat exchanger can be usually simplified with two manifolds (one inlet dividing manifold and an outlet combining manifold) and the heat transfer takes places only at the flow passages rather than at the manifolds. Because of the reverse flow direction, the hot side inlet (CO₂ side) shown in Figure 1(b) is designated at the upper left whereas the lower right represents its outlet.

Balanced Equations

Equations used in this research is based on the formulation of a U-type PHE by Bassiouny and Martin [15]. Although the basic formulation by Bassiouny and Martin can well apply to most of the working fluids, it may not totally fit into the present supercritical CO₂ plate heat exchanger. Some minor corrections are modified as described in the following. Taking cold side for example, the control volume of the grid node is shown in Fig. 2. Yet the corresponding momentum and mass balance equation can be written as in the following.

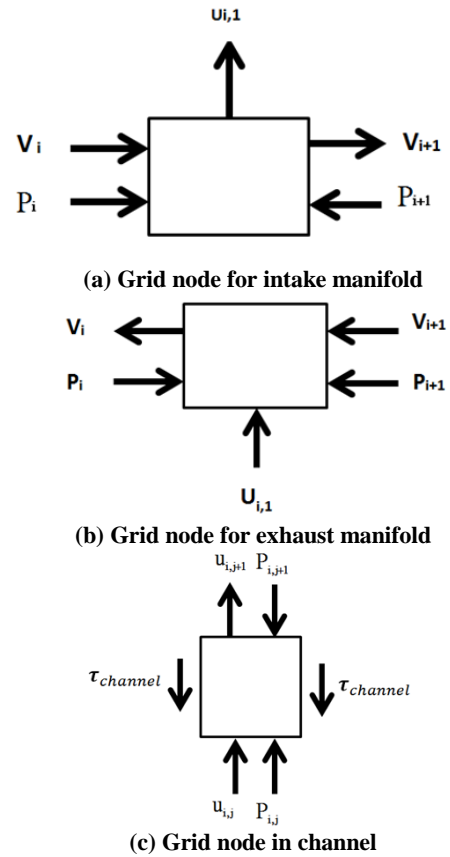


Fig. 2 Schematic for the control volume used for simulation in the intake, exhaust, and plate channels.

Equations:

(1) Intake manifold:

(i) Mass balance conservation

$$\rho_{in_i} AV_{in_i} = \rho A_c u_{i,1} + \rho_{in_{i+1}} AV_{in_{i+1}} \quad (1)$$

(ii) Momentum conservation

$$P_{in_i} A - P_{in_{i+1}} A = \rho AV_{in_{i+1}}^2 - \rho AV_{in_i}^2 + K_L \rho AV_{in_i}^2 \quad (2)$$

(2) Exhaust manifold:

(i) Mass conservation

$$P_{out_i} AV_{out_i} = \rho A_c u_{i,N} + \rho_{out_{i+1}} AV_{out_{i+1}} \quad (3)$$

(ii) Momentum conservation

$$P_{out_{i+1}} A - P_{out_i} A = \rho AV_{out_i}^2 - \rho AV_{out_{i+1}}^2 + K_c \rho AV_{out_{i+1}}^2 \quad (4)$$

(3) Channels:

(i) Mass conservation

$$\rho_{i,j} A_c u_{i,j} - \rho_{i,j+1} A_c u_{i,j+1} = 0 \quad (5)$$

(ii) Momentum conservation

$$P_{i,j} A_c - P_{i,j+1} A_c - \tau_w P l - \rho A_c u_{i,j}^2 + \rho A_c u_{i,j+1}^2 = 0 \quad (6)$$

Where

$$\tau_w = f_{c,i,j} \rho \left(\frac{u_{i,j}^2}{8} \right) \quad (7)$$

For the sake of simplicity, the terminologies of the symbol are described in the nomenclature. Besides, the turning loss into (or out of) plate channels should be taken into consideration.

$$P_{in_i} A - P_{ch,i} A_c + (1 + C_t) \rho_{i,1} A u_{i,1}^2 = 0 \quad (8)$$

$$P_{ch,N} A_c - P_{out_i} A + (1 + C_{to}) \rho_{i,N} A u_{i,N}^2 = 0 \quad (9)$$

For the energy balance equation, heat transfer in the manifolds is neglected. The corresponding equations are shown in the following [16]:

For cold side:

$$\begin{aligned} mc_{pHi} (T_{Hi,j+1} - T_{Hi,j}) &= \left(\frac{1}{A_w h_{Hi,j}} + \frac{\Delta x}{k A_w} + \frac{1}{A_w h_{Ci,j}} \right)^{-1} LMTD \\ &+ \left(\frac{1}{A_w h_{Hi,j}} + \frac{\Delta x}{k A_w} + \frac{1}{A_w h_{Ci+1,j}} \right)^{-1} LMTD \end{aligned} \quad (10)$$

For hot side:

$$\begin{aligned} mc_{pCi} (T_{Ci,j+1} - T_{Ci,j}) &= \left(\frac{1}{A_w h_{Hi,j}} + \frac{\Delta x}{k A_w} + \frac{1}{A_w h_{Ci,j}} \right)^{-1} LMTD \\ &+ \left(\frac{1}{A_w h_{Hi+1,j}} + \frac{\Delta x}{k A_w} + \frac{1}{A_w h_{Ci,j}} \right)^{-1} LMTD \end{aligned} \quad (11)$$

Where LMTD is the log mean temperature difference.

Mathematical formulation

In the simulation, the plate channel is first discretized into some tiny nodes and the foregoing mass, momentum, and energy equations in each node can be summarized in a matrix to form a system of nonlinear equations. The system nonlinear equations are then solved by Newton method along with Newton downhill algorithm for quicker convergence. Before the program starts, a curve fitting on thermal properties of water and CO₂ [12] should be made. Besides, the loss coefficients (such as K_L and K_c from Eqs. (2) and (4) subject to different configurations and flowrates are taken from reference [19]. Detailed flow chart depicting the solution algorithm for the plate heat exchanger is given in Fig. 3.

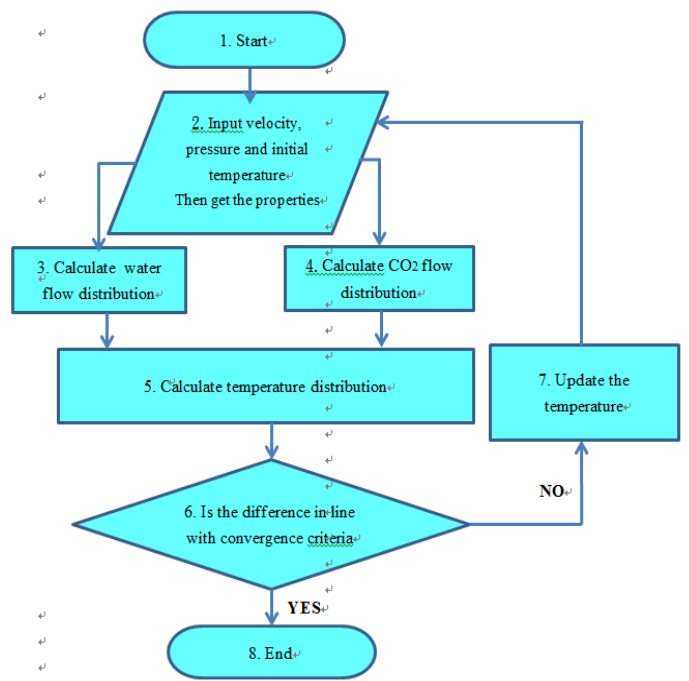
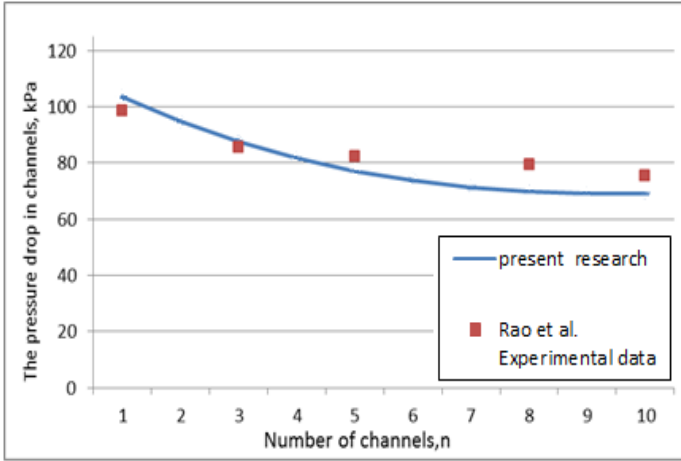


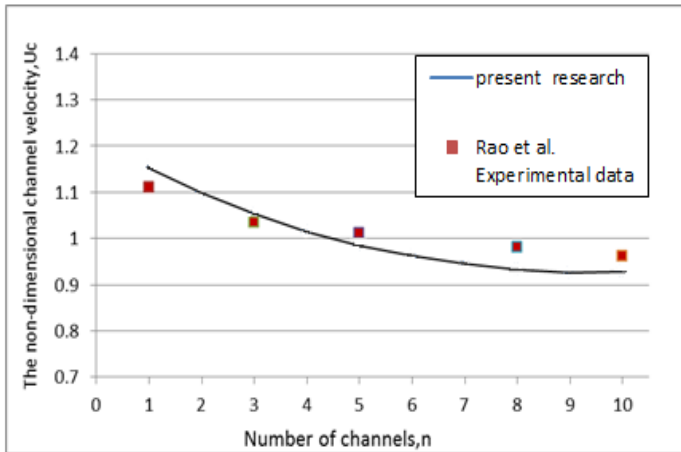
Fig. 3 Flow chart of the plate heat exchanger simulation program.

RESULTS AND DISCUSSION

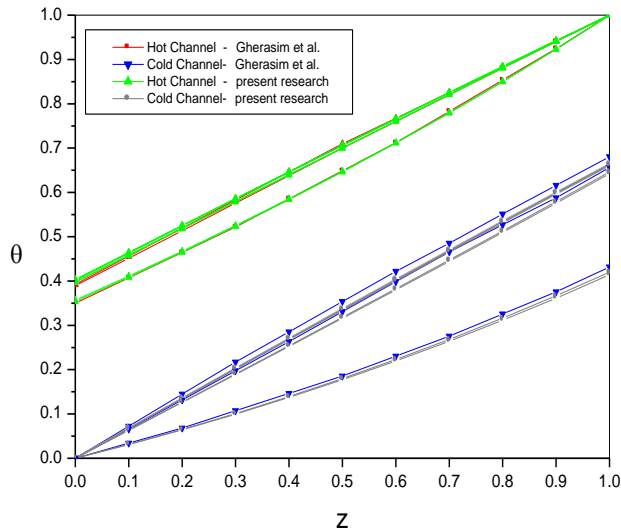
The proposed model is first compared with some existing data for validation. Fig. 4 is the comparison for the variation of the pressure drop and velocity distribution (in terms of $u_c = \frac{V_{ch}}{V_{chm}}$) between the predictive result and experimental data [20]. The inlet conditions and plate number is the same as those of [20]. Basically, the simulation is in line with the experimental data. Also, the calculation indicates that an appreciable falloff of pressure drop alongside the manifold. The results imply that there will be an uneven flow distribution alongside the plate. Apparently, the flowrate will decrease from the inlet toward the downstream due to detectable drop of pressure drop alongside the plate number. Fig. 4(a) and 4(b) is the comparison of the channel velocity between the predictive result and the experimental data from Rao et al. [20]. For the temperature distribution alongside the plate, comparison is also made with the simulation by Gherasim et al. [21] as shown in Fig. 4(c). Note that Gherasim et al. [21] performed a numerical simulation for plate heat exchanger using hot water and cold water. The current calculations are made with the same plate geometry and inlet conditions. Calculated results are shown in Fig. 4(c). Again, the prediction in this research also accord with the temperature distribution (dimensionless temperature) of Gherasim et al. [21]. The variation of the outlet temperature amid this study and theirs are within 1.5 °C (about 3%). Note that the detailed geometry and the correlations for the plate heat exchangers are given in Table 1.



(a) Comparison for pressure distribution with experimental data from Rao et al. [20]



(b) Comparison for velocity distribution from Rao et al. [20]



(c) Comparison for temperature distribution alongside the plate with field Gherasim et al. [21].

Fig. 4 Comparisons with the present predictive results with other researchers.

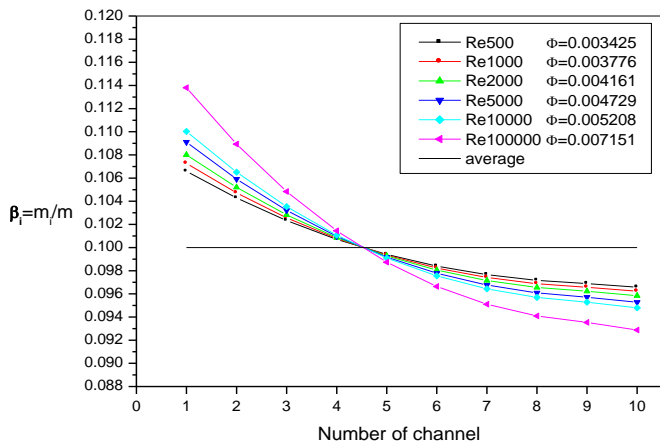
Table 1 Geometry of the plate heat exchanger tested by Gherasim et al. [21]

Geometry and inlet conditions for the plate heat exchanger	
Number of plates in cold side (n)	10
Number of plates in hot side	9
Plate spacing (mm)	2.9
Plate thickness (mm)	0.8
Height of plate (mm)	600
Width of plate (mm)	218
Inlet manifold diameter (mm)	70
Characteristics dimension of plate channel (mm)	5.8
Heat capacity ratio (C^*)	1
Both Water to water conditions at the inlet	
Inlet cold water velocity (m/s)	0.535
Inlet hot water velocity (m/s)	0.522
Inlet cold water temperature (K)	353
Inlet cold water temperature (K)	303
Correlation used for estimation of pressure drops and heat transfer [20]	
Friction Factor correlation	$f = 1.441 \cdot Re^{-0.206}$
Nusselt Number correlation	$Nu = 0.3 \cdot Re^{0.663} \cdot Pr^{0.333} \cdot (\mu / \mu_m)^{0.17}$

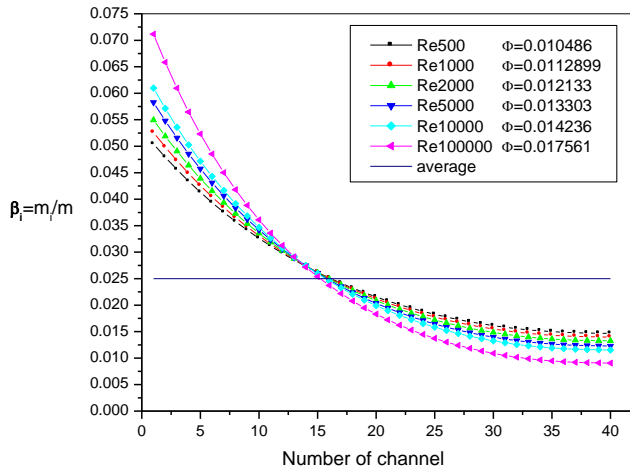
The foregoing results are applicable for water to water plate heat exchanger. For the present CO₂-water gas cooler, Fig. 5 indicates the effect of the Reynolds number on the mal-distribution of the flow under the isothermal state for water side. The plate numbers are 10 and 40, respectively. As shown in the figure, the flow mal-distribution increases with the rise of the Reynolds number. The results indicate that a higher inlet velocity leads to a severe mal-distribution alongside the plate. For an inlet Reynolds number of 100,000, the first plate may possess 21% higher mass flowrate than that in the last plate for n = 10. The higher mass flowrate near the entrance is mainly associated with larger pressure difference between the inlet and outlet conduit based on the calculated results. It is interesting to know that the mal-distribution becomes more and more pronounced when the number of plates increases further. In fact, difference in the mass flowrate between the first and last plate may exceed over seven times for an inlet Reynolds number of 100,000 when n = 40.

The foregoing velocity distribution for water side is made under isothermal condition. For the simulation of the CO₂-water gas cooler, until now, there were no heat transfer and friction correlation applicable for the supercritical CO₂. Hence the dimensionless correlation applicable for water shown in Table 1 from [20] is presumed valid and is used throughout this study.

Additionally, the plate geometry is the same as shown in Table 1. However, the local gigantic change of properties of CO₂ is taken into account in the calculation alongside the plate when using the correlation during iterations. This is especially important for CO₂. With imposing heat exchange between water and CO₂, the corresponding velocity distributions for water side and CO₂ side (the inlet water flowrate is 2 kg/s at 283 K and the inlet CO₂ flowrate is 6.15 kg/s at 370 K, and pressure is 8 MPa) subject to different values of C* (C_{CO₂} / C_{H₂O}) is shown in Fig. 6. For water, imposing heat exchange poses only a slight effect on the flow distribution at the first and last plate. This is because a significant difference in heat transfer rate occurring at these two plates since one side of the plate is insulated. Hence the effective viscosity increases and consequently a lower water velocity prevails. Yet the last plate experiences an even pronounced drop of velocity due to a larger temperature difference. For the rest of the plates of the cold water side, the flow distribution is analogous to those without heat transfer (Fig. 5). The results suggest that imposing heat transfer casts very minor influence on the water side velocity distribution. This is applicable for C* ranging from 0.1 to 1.

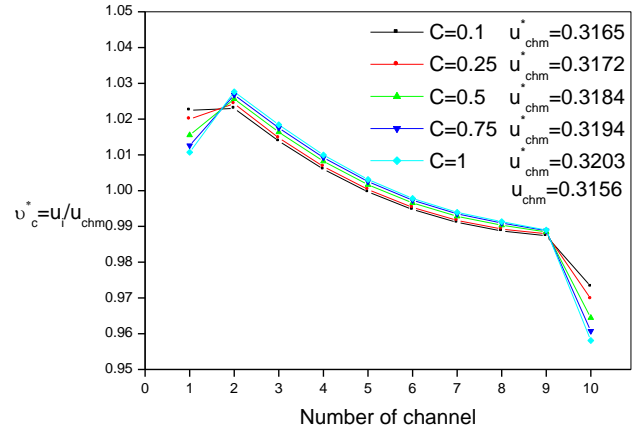


(a) n = 10

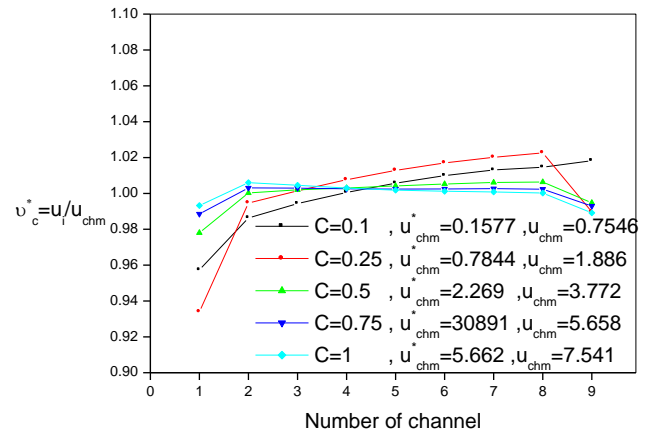


(b) n = 40

Fig. 5 Effects of Reynolds number on velocity distribution for water under isothermal state.



(a) water



(b) CO₂

Fig. 6 Velocity distributions of each plate for the water and CO₂.

The distribution of dimensionless velocity on CO₂ side is given in Fig. 6(b). However, it is clear from the figure that the distribution of CO₂ differs significantly from that of water. As appeared in Fig. 6(a), the water velocity distribution shows a consistent decline alongside the plate (except the first one due to considerable heat transfer difference). For CO₂ plate and C* = 1, it is found that the flow distribution is rather uniform, yet some mal-distribution emerges when C* is decreased. The flow distribution is actually associated with the pressure difference at the intake and outlet manifold. Based on the calculated results, it appears that the pressure difference between the intake and exhaust manifold is quite even alongside the manifold direction. In this regard, one can see the flow distribution is quite uniform for C* = 1. With C* being decreased to 0.1, the velocity difference is only around 6%. One of the explanations of the more uniform distribution of the CO₂ channels is for being operated at a very extremely high pressure. The results imply that the frictional pressure drop across the plate channel is much lower than the corresponding system pressure, thereby a better uniformity of the CO₂ is achieved. As C* is reduced, it appears

that the CO_2 may pass through the pseudo-critical temperature, leading to an appreciable change of properties such as heat capacity, density, and the like. As a consequence, the drastic change of property leads to change of heat transfer performance and its interaction with the water side leads to a comparatively uneven flow distribution as compared to that of $C^* = 1$. Note that at $C^* = 1$, the exit temperature of CO_2 is around 330 K which is still above the pseudo-critical temperature. Hence the property change is much small and accordingly its influence on velocity is relatively small.

Fig. 7 represents different results of heat transfer rate with different values of C^* (case 1 for 0.1, case 2 for 0.25, case 3 for 0.5, case 4 for 0.75 and case 5 for 1). The heat transfer rate rises with the C^* . By comparison between $C^* = 0.1$ (denote case 1 in Fig. 7) and $C^* = 0.5$ (case 3), we can find that the flow rate of CO_2 has risen fivefold while the heat transfer rate has increased nearly threefold. The significant rise of heat transfer rate suggests that the control resistance falls in the CO_2 side. Moreover, the heat transfer performance is considerably improved for the operation may pass through the pseudo-critical point.

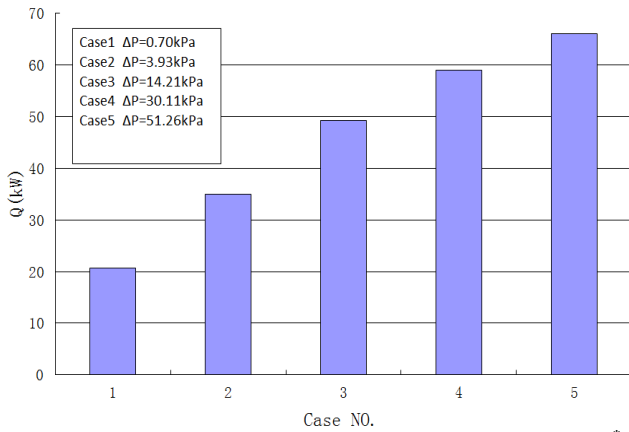
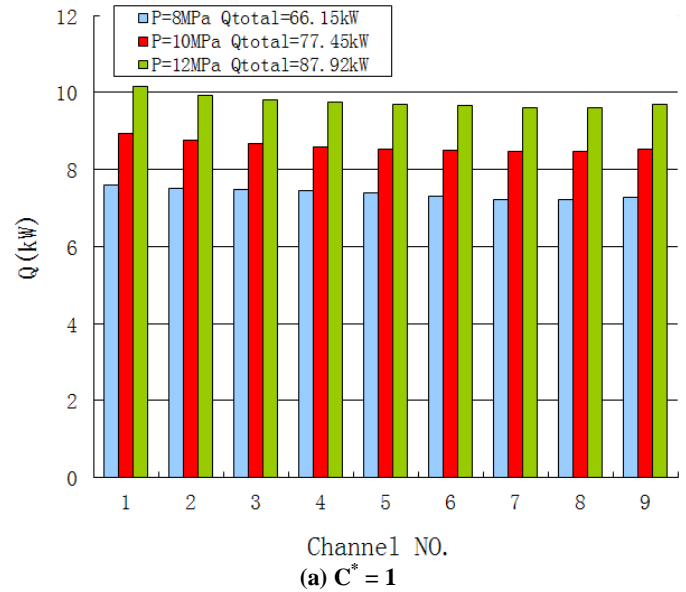


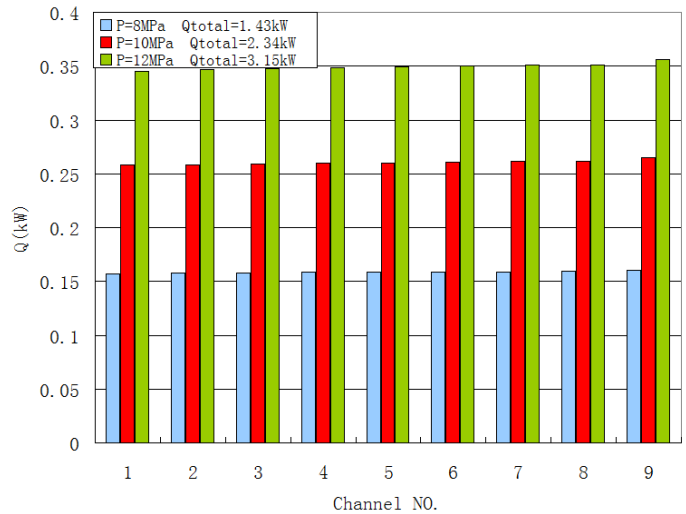
Fig. 7 Heat transfer rate distribution with different values of C^* .

The effect of inlet pressure of CO_2 on the total heat transfer rate for an inlet $C^* = 1$ and $C^* = 0.002$ are depicted in Fig. 8. Basically the heat transfer rate rises with the rise of inlet pressure. For $C^* = 1$ as shown Fig. 8(a), one can see that the total heat transfer rate increases with the rise of inlet pressure. This is somewhat expected for the effective heat capacity alongside the plate for a larger system pressure like $P = 12$ MPa is higher than that of $P = 10$ MPa as shown in Fig. 10(a). Basically, the outlet temperature of CO_2 is higher than the corresponding pseudo-critical temperature. In this sense, there is no significant change of heat capacity and the heat transfer coefficient. As a consequence, one can expect a moderate increase of heat transfer rate with the rise of system pressure. Thus, for $C^* = 0.002$ as shown in Fig. 8(b), one can see that the heat transfer rate of 12MPa is expected higher than that of 10MPa. As shown in Fig. 9, however, the heat flux of 12MPa is

slightly increased with the change of location along the plate but followed by a slight decline. Conversely, the heat flux of 8 MPa shows a noticeable increase after $x/L > 0.5$ which is different from the other two cases.



(a) $C^* = 1$



(b) $C^* = 0.002$

Fig. 8 Heat transfer rate for each CO_2 plate.

Basically, the phenomenon is associated with the transcritical phenomenon of CO_2 . Note that the heat capacity of CO_2 will undergo a tremendous increase when the temperature is near the pseudo critical temperature. Yet this phenomenon becomes more pronounced when the system pressure is close to the critical pressure. In this regard, it is expected that the pseudo-critical temperature may occur somewhere in the plate channel when C^* is reduced, see Fig. 10 for the heat capacity variation subject to various system pressure. Therefore, a gigantic rise of heat capacity as shown in Fig. 10(b) is encountered. Note that the abscissa in Fig. 10 represents the

location along the plate (A total of 10 grids are used in each plate for this simulation). On the other hand the sharp rise of heat capacity will follow by a sharp decline. Hence the substantial rise of heat capacity does not ensure an effective rise of average heat capacity. If the average heat capacity in the plate is higher than the average value at a high pressure such as in Fig. 10(b), one would expect an appreciable heat flux recovery at $P = 10$ MPa at some specific position within the plate. In the meantime, despite a sharp rise of heat capacity also emerges for $P = 8$ MPa, but again a sharp decline is also encountered when CO_2 flow is passing through the pseudo-critical point where the corresponding average heat capacity may be still lower than that of higher pressure, thereby a lower heat transfer rate prevails. The corresponding heat capacity for $C^* = 1$ for $P = 8$ MPa, 10 MPa and 12 MPa is shown in Fig. 10(a). As seen in the figure, the CO_2 flow did not pass through the pseudo-critical point, and as a result a continuous rise of heat transfer rate vs. system pressure is shown.

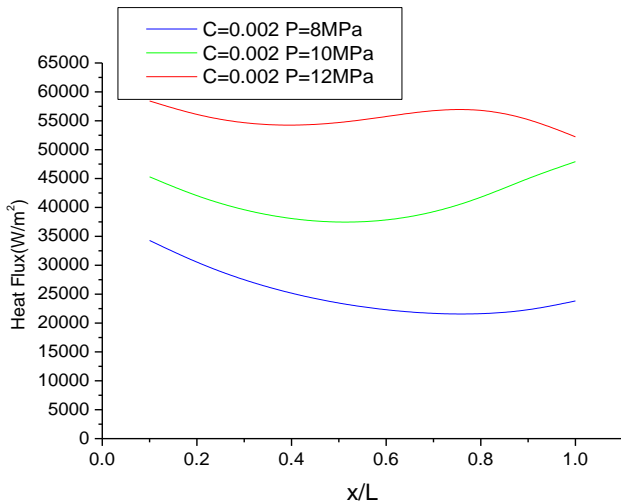
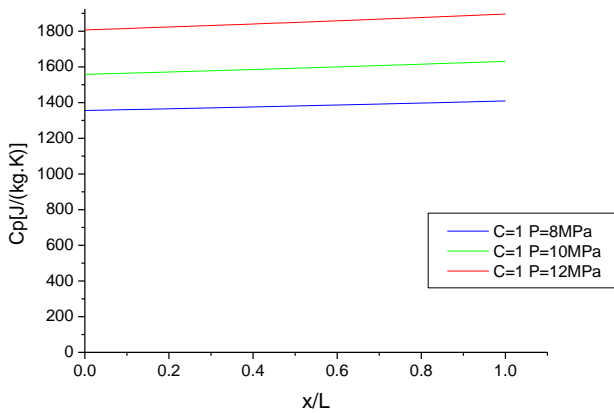
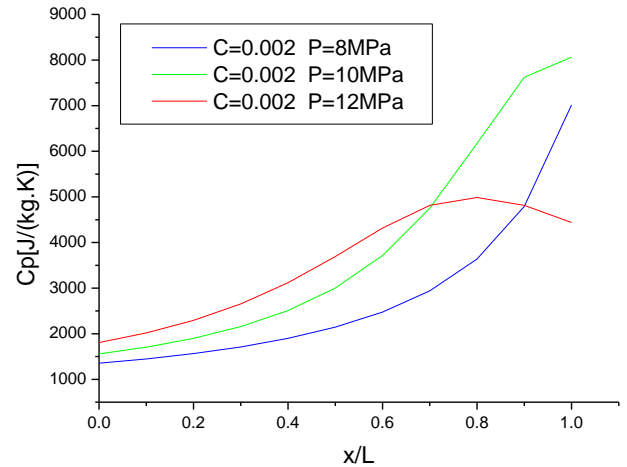


Fig. 9 Heat flux of CO_2 alongside the plate channel for $P = 10$ MPa and 12 MPa $C=0.002$.



(a) $C^* = 1$



(b) $C^* = 0.002$

Fig. 10 Heat capacity of CO_2 alongside the plate channel for $P = 10$ MPa and 12 MPa.

CONCLUSIONS

In this study, a plate heat exchanger model capable of handling supercritical like CO_2 had been proposed. The plate heat exchanger is of U-type configuration, the plate spacing is 2.9 mm and the plate thickness is 0.8 mm. The size of the plate is 600 mm wide and 218 mm in height. The proposed model takes into account the influence gigantic property change of CO_2 . Simulations are carried out for both isothermal and non-isothermal cases and were compared with some existing data for water-to-water plate heat exchangers. Based on the foregoing discussions, the following conclusions are made.

1. The proposed model was first compared with some existing water to water plate heat exchanger data. Generally, the predicted water flow distributions are in line with the experimental data. Yet the simulation results of temperature distribution alongside the plate also agree excellently with other predicted model.
2. For the plate heat exchanger in the water side, it is found that a detectable mal-distribution is found in associated with the inlet flowrate at the manifold. Basically, larger mal-distribution is encountered when the inlet flowrate is increased. In addition, the mal-distribution also increases with the rise of plate number. In the worst case, a seven-fold difference can be encountered between the first and last plate. Normally the largest flowrate occurs at the first plate. However, with imposing heat transfer, the flow rate at the first plate may be slight reduced due to the uneven heat transfer rate at the first plate.
3. The simulation indicates that the inlet temperature of water casts negligible influence on the water flowrate distribution. This is because the density variation for water is quite small

with the temperature. By contrast, it is found that the inlet temperature difference for the CO₂ side may raise significant change of thermodynamics and transport property of CO₂, and result in a great difference in flow distribution. For the water side, it is found that the flowrate normally declines alongside the manifold. However, the flowrate distribution of CO₂ is rather uniform due to its much higher system pressure. However, the flow distribution of CO₂ also depends on C*, smaller C* may reverse the flow distribution to increasing trend rather commonly observed decreasing trend despite the variation from plate to plate is still quite small.

ACKNOWLEDGMENTS

The financial support from the Ministry of Science and Technology, Taiwan is highly appreciated.

REFERENCES

- [1] Khan, T. S., M.S. Khan, M.S., Chyu, M.C., Ayub, Z.H., Chattha, J.A., "Review of heat transfer and pressure drop correlations for evaporation of fluid flow in plate heat exchangers," *HVAC&R Research*, 15(2), pp. 169-188, (2009).
- [2] Khan, T. S., M.S. Khan, M.S., Chyu, M.C., Ayub, Z.H., "Experimental investigation of single phase convective heat transfer coefficient in a corrugated plate heat exchanger for multiple plate configurations," *Applied Thermal Engineering*, 30, pp. 1058-1065, (2010).
- [3] Han, W., Saled, K., Aute, V., Ding, G., Hwang, Y., Radermacher, R., "Numerical simulation and optimization of single-phase turbulent flow in chevron-type plate heat exchanger with sinusoidal corrugations," *HVAC&R Research*, 17(2), pp. 186-197, (2011).
- [4] Hashimoto K., "Technology and market development of CO₂ heat pump water heaters (ECO CUTE) in Japan," *IEA Heat Pump Centre Newsletter*, 12-16 (2006).
- [5] ASHRAE Handbook, Refrigeration (2010). ASHRAE, Atlanta, GA.
- [6] Lorentzen, G., Pettersen J., "A new, efficient and ambientally benign system for car air conditioning," *Int. J. Refrigeration*, 16, pp. 4-12 (1993).
- [7] Lorentzen, G., "Revival of carbon dioxide as a refrigerant," *Int. J. Refrigeration*, 17, pp. 292-300, (1994).
- [8] Lorentzen, G., "The use of natural refrigerant: a complete solution to the CFC/HCFC predicament," *Int. J. Refrigeration*, 18, pp. 190-197, (1994).
- [9] Qi, P.C., He, Y.L., Wang, X.L., Meng, X.Z., "Experimental investigation of the optimal heat rejection pressure for a transcritical CO₂ heat pump water heater," *Applied Thermal Engineering*, 56, pp. 120-125, (2013).
- [10] Dittus, F.W., Boelter, L.M.K., "Heat transfer in automobile radiators of the tubular type," *Univ. Calif. Publ. Eng.*, 2(13), pp. 443-46, (1930).
- [11] Gnielinski, V., "New equations for heat and mass transfer in turbulent pipe and channel flow," *International Chemical Engineering*, 16, pp. 359-368 (1976).
- [12] McLinden, M. Klein, S.A., Lemmon, E.W., Peskin, A.P., "Thermodynamic and Transport properties of Refrigerants and Refrigerant Mixtures-REFPROP," Version 8.0, National Institute of Standards and Technology, USA, (1998).
- [13] Yoon, S.H., Kim, J.H., Hwang, Y.W., Kim, M.S., Min, K., Kim, Y., "Heat transfer and pressure drop characteristics during the in-tube cooling process of carbon dioxide in the supercritical region," *International Journal of Refrigeration*, 26, pp. 857-864, (2003).
- [14] Son, C.H., Park, S.J., "An experimental study on heat transfer and pressure drop characteristics of carbon dioxide during gas cooling process in a horizontal tube," *International Journal of Refrigeration*, 29, pp. 539-546, (2005).
- [15] Bassiouny, M K., Martin, H., "Flow distribution and pressure drop in plate heat exchangers-I," *Chemical Engineering Science*, 39(4), pp. 693-700, (1984).
- [16] Rao, B.P., Kumar, P.K., Das, S.K., "Effect of flow distribution to the channels on the thermal performance of a plate heat exchanger," *Chemical Engineering and Processing*, 41, pp. 49-58, (2002).
- [17] Yu, P.Y., Lin, K.H., Lin, W.K., Wang, C.C., "Performance of a tube-in-tube CO₂ gas cooler," *Int. J. of Refrigeration*, 35, pp. 2033-2038 (2012).
- [18] Yu, P.Y., Lin W.K., Wang, C.C., "Performance evaluation of a tube-in-tube CO₂ gas cooler used in a heat pump water heater," *Experimental Thermal and Fluid Science*, 54, pp. 304-312, (2014).
- [19] Idelchik, I.E., "Handbook of Hydraulic Resistance," pp. 413-501, 3rd Edition, New York, (1994).
- [20] Rao, B.P., Sunden, B., Das, S.K., "An experimental investigation of the port flow maldistribution in small and large plate package heat exchangers," *Applied Thermal Engineering*, 26, pp. 1919-1926, (2006).
- [21] Gherasim, I., Galanis, N., Nguyen, C.T., "Effects of dissipation and temperature-dependent viscosity on the performance of plate heat exchangers," *Applied Thermal Engineering*, 29, pp. 3132-3139, (2009).